Journal of Physics A: Mathematical and Theoretical

PAPER • **OPEN ACCESS**

Resetting dynamics in a confining potential

To cite this article: R K Singh *et al* 2020 *J. Phys. A: Math. Theor.* **53** 505003

OPEN ACCESS
IOP Publishing
Journal of Physics A: Mathematical and Theoretical
J. Phys. A: Math. Theor. **53** (2020) 505003 (28pp)
https://doi.org/10.1088/1751-8121/abc83a

Resetting dynamics in a confining potential

R K Singh[1], R Metzler[2,*] and T Sandev[2,3,4]

[1] Department of Physics, Ramakrishna Mission Vivekananda Educational and Research Institute, Belur Math, Howrah 711202, India
[2] Institute of Physics & Astronomy, University of Potsdam, D-14776 Potsdam-Golm, Germany
[3] Research Centre for Computer Science and Information Technologies, Macedonian Academy of Sciences and Arts, Bul. Krste Misirkov 2, 1000 Skopje, Macedonia
[4] Institute of Physics, Faculty of Natural Sciences and Mathematics, Ss. Cyril and Methodius University, Arhimedova 3, 1000 Skopje, Macedonia

E-mail: rksinghmp@gmail.com, rmetzler@uni-potsdam.de and trifce.sandev@manu.edu.mk

Received 3 September 2020, revised 30 October 2020
Accepted for publication 6 November 2020
Published 25 November 2020

Abstract

We study Brownian motion in a confining potential under a constant-rate resetting to a reset position x_0. The relaxation of this system to the steady-state exhibits a dynamic phase transition, and is achieved in a light cone region which grows linearly with time. When an absorbing boundary is introduced, effecting a symmetry breaking of the system, we find that resetting aids the barrier escape only when the particle starts on the same side as the barrier with respect to the origin. We find that the optimal resetting rate exhibits a continuous phase transition with critical exponent of unity. Exact expressions are derived for the mean escape time, the second moment, and the coefficient of variation (CV).

Keywords: diffusion, resetting, barrier escape, first-passage

(Some figures may appear in colour only in the online journal)

1. Introduction

The first-passage time measures the time of first-crossing of a preset value x_0 for a process $x(t)$ [1]. For continuous processes this time is equivalent to the time of first-arrival or first-hitting [2]. The concept of first-passage time plays a central role in the description of molecular reaction

*Author to whom any correspondence should be addressed.

[1, 3–5], specifically in gene regulation [6–9], as well as in animal search and random target search processes [10–12] and disease spreading [13, 14], to name but a few applications. A particular form of the first-passage time concept is the scenario of barrier crossing, in which a particle starts in a potential well, and the escape time up to a given point x_0 away from the starting position is sought [15, 16]. Barrier crossing is an intrinsic process in chemical reactions, during which typically an activation energy barrier needs to be crossed [17]. In this scenario the approach to the target, typically represented by an absorbing boundary condition or a δ-sink [2], in the crossing dynamics is suppressed by an Arrhenius–Boltzmann factor, for instance, seen in the Kramers rate $r \propto \exp(-\beta\Delta V)$ for barrier crossing, where $\beta/(k_{\rm B}T)$ is the Boltzmann factor at temperature T and ΔV is the potential energy difference needed to be overcome by the test particle [16].

Restart is a natural step in many search processes, and it is one of the go-to steps which is taken every now and then. For instance, a foraging bumblebee or a hunting group of lions regularly return to their nest or water hole. Humans searching for an item also often restart their search. A natural question that arises in this context is whether restarts expedite the completion of the search process, or rather tend to delay it. This strategy of intermittent search with restart has decades of history ranging from stochastic algorithms [18–20], chemical reactions [21], human behaviour [22], foraging [23], polymer translocation [24], catastrophes in population dynamics [25–27], but also queueing theory [28, 29], etc. Given the ubiquity of random search processes arising in natural and artificial settings the significance of restarts in completion of search processes cannot be overemphasised.

Especially in the context of stochastic processes and random searches the term 'resetting' or 'stochastic resetting' has become a standard term. Resetting has been extensively studied in the physics literature and continues to date to be one of the most researched topics in nonequilibrium statistical physics [30]. For example, a one-dimensional Brownian motion continues to grow in space, in that the width of the Gaussian position distribution grows with time as $\sqrt{t}$. As a consequence, the system does not relax. However, when resetting is introduced, pulling the Brownian particle back to its initial position every now and then, the system relaxes to a nonequilibrium steady state [31]. Resetting not only affects relaxation, it also has significant effects on the first-passage properties of a Brownian particle. Continuing with the example of one-dimensional Brownian motion, but now on a semi-infinite line, the mean escape time to the absorbing boundary is infinity [1]. However, resetting causes the mean time to escape to be finite [31]. Furthermore, there exists an optimal resetting rate at which the mean escape time is minimal, and for that value of the resetting rate the relative standard deviation of the first passage times is unity, a universal feature of optimally restarted processes [32].

The fact that a system evolves via its natural dynamics between two resetting events leads to a fundamental relation between the completion times in the presence of resetting to that in the absence of any resetting. This observation has been demonstrated on multiple occasions when addressing diffusion under stochastic resetting [33–41], specifically including resetting on comb-like structures [42, 43], scaled Brownian motion with resetting [44], random search for several targets under resetting [45], and diffusion processes with non-instantaneous resetting [46, 47]. In addition to representing a random walk-mediated search and a nonequilibrium process, diffusion under resetting also connects to one of the most central topics in equilibrium statistical physics, namely, critical phenomena [48–53]. This observation has been exemplified on numerous instances in the resetting literature [54–57].

The significance of the connection between the properties of a stochastic process with and without reset lies in the fact that resetting expedites the completion of a process only if its counterpart in the absence of resetting exhibits significant fluctuations in the statistics of first passage times [58] (compare [59] and below). In other words, resetting is useful if and only if

the coefficient of variation (CV), the relative standard deviation of the first-passage times, in the absence of resetting is greater than unity [60]. Notwithstanding the universal laws governing stochastic dynamics under reset, specific cases addressing Brownian motion in a potential under reset have been relatively few, for example, diffusive motion under reset in presence of a drift [61], a logarithmic potential [62], confining potential [63], harmonic potential [64], etc. One of the most interesting cases of Brownian motion in a potential well is a piecewise linear potential well [65]. The primary advantage of the piecewise linear potential scenario lies in its mathematical simplicity, making it fully tractable analytically. Furthermore, the problem of Brownian motion in a potential well connects to the pioneering work of Kramers' in the above-mentioned barrier crossing scenario [15], and it addresses rates of chemical reactions [17, 66], which further was extended to problem with anomalous kinetics [67, 68]. And with resetting being an integral entity in many chemical reaction systems, for example, the renowned Michaelis–Menten reaction scheme [69, 70], the question of addressing the effects of resetting on Brownian motion in a potential well becomes very relevant. Motivated by this observation, we address in this paper the problem of a Brownian motion in a piecewise linear potential subject to constant rate resetting. One of the main results of this work is that resetting aids in barrier escape if and only if the reset location lies on the same side as the barrier. Moreover, we demonstrate that the optimal resetting rate shows a continuous phase transition with critical exponent of unity.

The paper is organised as follows: in section 2 we study the statistics of a Brownian motion moving in a piecewise linear confining potential, and look at both its transient and steady state behaviour under resetting. In the following section 3, we look at the transition to the steady state, i.e., starting with a given location and knowing the steady state of the problem, how does the system relax to its long-time limit? We find that there is a light cone region in space time in which the steady state is achieved, and the size of this region grows linearly in time. Next we move on to the Kramers' problem under resetting in section 4, where we analyse the corresponding system in the absence of resetting and assess the domain of parameter space in which resetting can expedite the barrier crossing. Finally, we summarise our findings in section 5.

2. Resetting dynamics in a potential

For a Brownian motion in a potential $V(x)$ the Fokker–Planck equation describing the dynamics of the probability density function (PDF) $p_r(x,t)$ under a constant resetting rate r reads [36, 71, 72]

$$\frac{\partial}{\partial t}p_r(x,t) = \left(\frac{\partial}{\partial x}V'(x) + D\frac{\partial^2}{\partial x^2}\right)p_r(x,t) - rp_r(x,t) + r\delta(x-x_0), \tag{1}$$

where here we choose the potential function to be the piecewise linear function

$$V(x) = \begin{cases} -U_0 x, & x \leqslant 0 \\ U_0 x, & 0 \leqslant x \end{cases}, \tag{2}$$

in the above equations $U_0 > 0$, and $x = x_0 > 0$ is the location of reset. Here we assume that the particle is reset to its initial position x_0 with a constant rate r (the times between two consecutive resetting events are taken from an exponential distribution with mean $1/r$). Each resetting event to the initial position x_0 renews the process at a rate r, i.e., between two consecutive renewal events, the particle undergoes diffusion in the non-monotonic potential (2). The third term on

the right-hand side of equation (1) represents the loss of probability from the position x due to reset to the initial position x_0, while the fourth term is the gain of probability at x_0 due to resetting from all other positions.

2.1. Solution in Laplace domain

The Fokker–Planck equation (1) in Laplace domain reads

$$s\tilde{p}_r(x,s) - p_r(x,0) = \left(\frac{\partial}{\partial x}V'(x) + D\frac{\partial^2}{\partial x^2}\right)\tilde{p}_r(x,s) - r\tilde{p}_r(x,s) + \frac{r}{s}\delta(x-x_0), \tag{3}$$

with $p_r(x,0) = \delta(x-x_0)$, where $\tilde{p}_r(x,s) = \mathscr{L}\{p_r(x,t)\}(s) = \int_0^\infty p_r(x,t)\exp(-st)\mathrm{d}t$ is the Laplace transform pair of $p_r(x,t)$. The solution to the above equation reads

$$\tilde{p}_r(x,s) = \begin{cases} a_+\mathrm{e}^{m_+x}, & x \leqslant 0, \\ b_+\mathrm{e}^{-m_+x} + b_-\mathrm{e}^{-m_-x}, & 0 \leqslant x \leqslant x_0, \\ c_+\mathrm{e}^{-m_+x}, & x_0 \leqslant x, \end{cases} \tag{4}$$

where $m_\pm = \frac{U_0}{2D}(1 \pm \Delta_{r+s})$ are the roots of the auxiliary equation $0 = m^2 - \frac{U_0}{D}m - \frac{r+s}{D}$, and

$$\Delta_{r+s} = \sqrt{1 + \frac{4D(r+s)}{U_0^2}}. \tag{5}$$

Now, continuity of the solution at the points $x = 0$ and $x = x_0$, i.e., $\lim_{x\to 0^+}\tilde{p}_r(x,s) = \lim_{x\to 0^-}\tilde{p}_r(x,s)$ and $\lim_{x\to x_0^+}\tilde{p}_r(x,s) = \lim_{x\to x_0^-}\tilde{p}_r(x,s)$ fixes two relations between the parameters,

$$a_+ = b_+ + b_-, \tag{6a}$$

$$c_+ = b_+ + b_- \ \exp([m_+ - m_-]x_0). \tag{6b}$$

In addition to the continuity of the solution at the resetting point and turning point of the potential, the derivative of $\tilde{p}(x,s)$ exhibits a discontinuity at the two points. Firstly, the discontinuity at the origin arises due to the singular nature of the potential at the turning point and is obtained by integrating equation (3), yielding

$$0 = \left(\frac{\partial}{\partial x}\tilde{p}_r(x,s)\bigg|_{0+} - \frac{\partial}{\partial x}\tilde{p}_r(x,s)\bigg|_{0-}\right) + \frac{1}{D}\left(V'(x)\tilde{p}_r(x,s)|_{0+} - V'(x)\tilde{p}_r(x,s)|_{0-}\right), \tag{7}$$

such that

$$2\left(m_+ - \frac{U_0}{D}\right)b_+ = \left(\frac{2U_0}{D} - (m_+ + m_-)\right)b_-. \tag{8}$$

The nature of the discontinuity at the initial location $x = x_0$ is, however, different, as it is not due to the singular nature of the potential at the origin but arises due to the degenerate nature

of the distribution at $t = 0$,

$$0 = \left(\frac{\partial}{\partial x} \tilde{p}_r(x,s)\Big|_{x_0^+} - \frac{\partial}{\partial x} \tilde{p}_r(x,s)\Big|_{x_0^-} \right) + \frac{1}{D} \left(V'(x)\tilde{p}_r(x,s)|_{x_0^+} V'(x)\tilde{p}_r(x,s)|_{x_0^-} + \frac{r+s}{sD}, \right.$$

$$\Rightarrow b_- = \frac{r+s}{sD} \frac{\mathrm{e}^{m_- x_0}}{m_+ - m_-}. \tag{9}$$

Inserting the values of the parameters we have the solution for the PDF under resetting in Laplace domain,

$$\tilde{p}_r(x,s) = \begin{cases} \dfrac{r+s}{s} \dfrac{1}{U_0(\Delta_{r+s}-1)} \exp\left[\dfrac{U_0}{2D}\{(x+x_0) + \Delta_{r+s}(x-x_0)\}\right], & x \leqslant 0, \\ \dfrac{r+s}{s} \dfrac{1}{U_0\Delta_{r+s}(\Delta_{r+s}-1)} \exp\left[\dfrac{U_0}{2D}\{(1-\Delta_{r+s})x_0 - x\}\right] & \\ \times \left[\Delta_{r+s} \exp\left(\dfrac{U_0 x \Delta_{r+s}}{2D}\right) - 2 \sinh\left(\dfrac{U_0 x \Delta_{r+s}}{2D}\right)\right], & 0 \leqslant x \leqslant x_0, \\ \dfrac{r+s}{s} \dfrac{1}{U_0\Delta_{r+s}(\Delta_{r+s}-1)} \exp\left[\dfrac{U_0}{2D}\{x_0 - (1+\Delta_{r+s})x\}\right] & \\ \times \left[\Delta_{r+s} \exp\left(\dfrac{U_0 x_0 \Delta_{r+s}}{2D}\right) - 2 \sinh\left(\dfrac{U_0 x_0 \Delta_{r+s}}{2D}\right)\right], & x_0 \leqslant x. \end{cases} \tag{10}$$

From the solution it is clear that two cusps are present, one at the origin ($x = 0$) due to the singular nature of the potential, and another one at the initial position (which is also the location of reset x_0), at which the first derivatives are discontinuous. Of course, this does not come as a surprise as resetting introduces a source of probability at x_0, which is reflected as a cusp in the stationary distribution. We see that when the location of the reset is shifted to the origin, the intrinsic symmetry of the problem with respect to inversion of axis is restored. This follows easily by substituting $x_0 = 0$ in result (10),

$$\tilde{p}_r(x,s) = \frac{r+s}{s} \frac{1}{U_0(\Delta_{r+s}-1)} \times \exp\left(-\frac{U_0}{2D}(1+\Delta_{r+s})|x|\right), \tag{11}$$

which in absence of potential reduces to the well-known result $\tilde{p}_r(x,s) = (2s)^{-1}\sqrt{(r+s)/D}\ \exp\left(-\sqrt{(r+s)/D}|x|\right)$. The Details of the solution for the symmetric case are provided in appendix A, and the asymmetric case follows similarly. Furthermore, the limiting form of the solutions $\tilde{p}_r(x,s)$ in the limit $s \to 0$ leads to the steady state of the system [71]. A graphical representation of solution (10) is shown in figure 1. From figures 1(a)–(c) one can see the transition dynamics to the steady state for different values of the resetting parameter r, where the black dotted lines corresponds to the time moment $t = 10$. These black dotted lines for $t = 10$ are exactly the same as the stationary distribution obtained in [71], as shown in figure 1(d). The two cusps of the PDF at the origin $x = 0$ and at the initial/resetting position x_0, whose appearance was discussed above, are clearly observed from the figure.

From solution (10) we calculate the mean squared displacement (MSD) $\langle x^2(t)\rangle = \int_{-\infty}^{\infty} x^2 p_r(x,t)\mathrm{d}x$, which in the Laplace domain reads

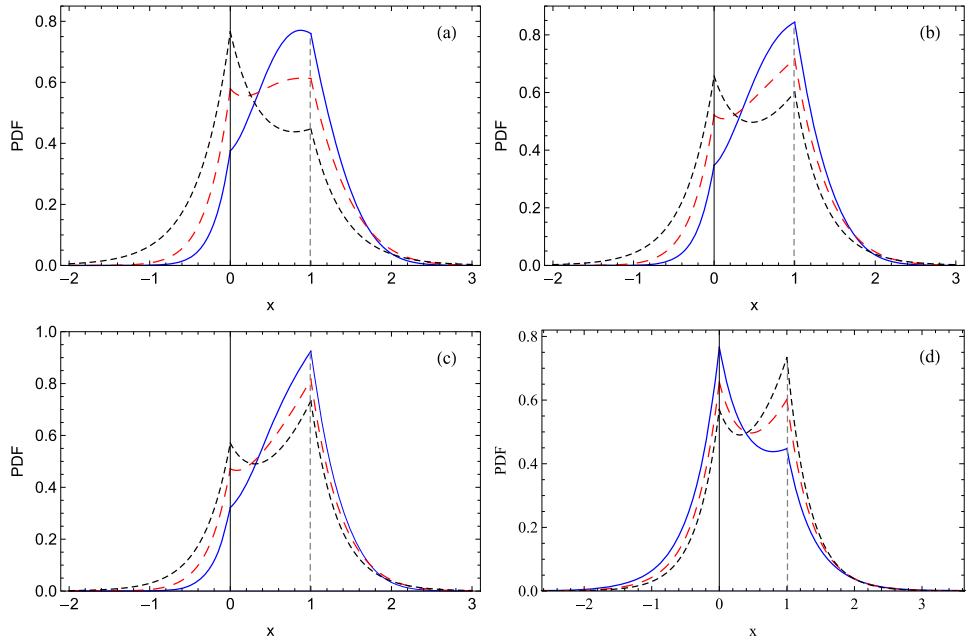

Figure 1. PDF (10) for $D = 0.5$, $U_0 = 1$, $x_0 = 1$, $t = 0.3$ (blue solid line), $t = 0.5$ (red dashed line), $t = 10$ (black dotted line), and (a) $r = 0.6$, (b) $r = 1$, (c) $r = 1.4$. Panel (d) corresponds to the stationary PDF for the case $D = 0.5$, $U_0 = 1$, $x_0 = 1$, and $r = 0.6$ (blue solid line), $r = 1$ (red dashed line), $r = 1.4$ (black dotted line) obtained in [71]—for $t = 10$, the PDF (10) already approaches these stationary distributions, as it should be for the long time limit. The PDFs are calculated using the numerical inverse Laplace transform algorithm in Mathematica [73].

$$\begin{aligned}\langle \tilde{x}^2(s)\rangle &= \int_{-\infty}^{0} x^2 \tilde{p}_r(x,s)\mathrm{d}x + \int_{0}^{x_0} x^2 \tilde{p}_r(x,s)\mathrm{d}x + \int_{x_0}^{\infty} x^2 \tilde{p}_r(x,s)\mathrm{d}x \\ &= \frac{x_0^2}{s} + \frac{2(D - U_0 x_0)}{s(r+s)} - \frac{U_0^2}{s(r+s)^2}\ \exp\left(\frac{U_0 x_0(1-\Delta_{r+s})}{2D}\right) \\ &\quad \times \left[1 + \Delta_{r+s} - 2\ \exp\left(-\frac{U_0\, x_0(1-\Delta_{r+s})}{2D}\right)\right]. \end{aligned} \tag{12}$$

From these general results we analyse the limiting cases of the MSD. For the symmetric case ($x_0 = 0$) equation (12) reduces to the expression

$$\langle \tilde{x}^2(s)\rangle = \frac{8D^2}{U_0^2} \frac{s^{-1}}{\left(\sqrt{1 + \frac{4D(r+s)}{U_0^2}} + 1\right)^2}, \tag{13}$$

and in absence of the potential to $\langle \tilde{x}^2(s)\rangle = \frac{x_0^2}{s} + 2D\frac{s^{-1}}{r+s}$, i.e., $\langle x^2(t)\rangle = x_0^2 + \frac{2D}{r}\left(1 - \mathrm{e}^{-rt}\right)$. The long time limit ($t \to \infty$, i.e., $s \to 0$) of (12) yields a saturation of the MSD,

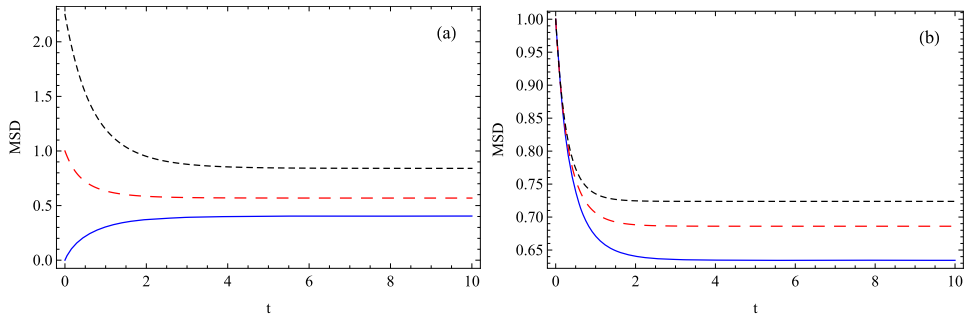

Figure 2. MSD (12) for (a) $r = 0.25$ and $x_0 = 0$ (blue solid line), $x_0 = 1$ (red dashed line), $x_0 = 1.5$ (black dotted line); (b) $x_0 = 1$ and $r = 0.6$ (blue solid line), $r = 1$ (red dashed line), $r = 1.4$ (black dotted line). We set $D = 0.5$, $U_0 = 1$.

$$\langle x^2(t)\rangle \sim x_0^2 + \frac{2(D - U_0\, x_0)}{r} - \frac{U_0^2}{r^2}\ \exp\left(\frac{U_0 x_0(1-\Delta_r)}{2D}\right) \times \left[1 + \Delta_r - 2\ \exp\left(-\frac{U_0 x_0(1-\Delta_r)}{2D}\right)\right], \tag{14}$$

which for $x_0 = 0$ turns into $\langle x^2(t)\rangle \sim r^{-2}\left[2Dr - U_0^2(\Delta_r - 1)\right]$, where the symbol $\sim$ means asymptotic equivalence. Here we apply the final value theorem $\lim_{t\to\infty}\langle x^2(t)\rangle = \lim_{s\to 0} s\langle\tilde{x}^2(s)\rangle$ to equation (12). A graphical representation of the MSD for different initial positions x_0 and different resetting rates is shown in figure 2, from where one observes the transition to the plateau in the long time limit.

3. Transition to the steady state

3.1. The symmetric case: $x_0 = 0$

Resetting to a fixed initial location introduces a nonequilibrium steady state in the system to which it relaxes in the long time limit. However, this relaxation is often far from trivial. The existence of a dynamical transition in the relaxation behaviour under resetting was addressed in [74]. As shown there the nonequilibrium steady state is established in an inner core region $[-\xi(t), \xi(t)]$ around the resetting point, which we take to be at the origin $x = 0$. Outside this core region the system is still transient. As the authors show the relaxation to the fixed point, in systems with $x \to -x$ symmetry, is conveniently captured by the length scale $x \sim \xi(t)$, defined in terms of the large deviation function (LDF) $I_{\rm r}(w)$,

$$p_r(x,t) \sim \exp\left(-t\, I_r\left(\frac{x}{\xi(t)}\right)\right), \tag{15}$$

while the length scale grows algebraically, $\xi(t) \sim t^{1/\nu}$, with the dynamical exponent ν. So the problem of addressing the relaxation to the steady state boils down to calculating the LDF for the problem. The LDF, also known as the rate function, is defined either in terms of the probability distribution of the stochastic process (cf equation (15)) or in terms of the generating function and Legendre transform (see, for example, references [30, 75]). The generating function formalism is particularly advantageous when looking at the asymptotic behaviour of additive functionals, such as the area traversed under a Brownian excursion.

However, in the present problem we are interested in the relaxation behaviour of the system under stochastic resetting, and hence, we evaluate the LDF following equation (15). To proceed with this analysis we employ the renewal equation [44, 76] connecting the density $p_r(x,t)$ in the presence of resetting with its counterpart in absence of resetting $p_0(x,t)$,

$$p_r(x,t) = \mathrm{e}^{-rt} p_0(x,t) + \int_0^t \mathrm{d}t' r\, \mathrm{e}^{-rt'} p_0(x,t'). \tag{16}$$

Here the first term describes the contribution to $p_r(x,t)$ of trajectories that have not been reset up to time t, while the second term is the contribution of resets to the PDF. Furthermore, the renewal equation makes it very conspicuous that the dynamical behaviour under resets is controlled by the density in the absence of any resettings. Now, for the problem under consideration

$$p_0(x,t) = \frac{U_0}{4D}\, \mathrm{e}^{-U_0|x|/2D} \left(1 + \frac{|x|/t}{U_0}\right) \mathrm{e}^{-t\Phi(1,x/t)}, \tag{17}$$

where $\Phi(1,x/t) = U_0^2/4D + x^2/4Dt^2$ is the saddle point approximation to the density profile (see appendix B for details), and we have made the additional assumption that the Brownian particle initially starts at the origin, $x_0 = 0$. Hence, the first term of the renewal equation (16) is already known. In order to assess the second term, we need to evaluate the integral of $p_0(x,t)$ modulated by the density of the reset intervals. It reads (see appendix B),

$$\begin{aligned}
\int_0^t \mathrm{d}t' r\, \mathrm{e}^{-rt'} p_0(x,t') &= t\int_0^1 \mathrm{d}\tau \left(1 + \frac{w/\tau}{U_0}\right) \mathrm{e}^{-t\Theta(\tau,w)} \\
&\approx t\frac{\sqrt{2\pi}(1 + w/U_0\tau_0)}{|t\Theta''(\tau_0,w)|^{1/2}} \mathrm{e}^{-t\Theta(\tau_0,w)} \\
&\sim \exp\left(-\frac{U_0}{2D}(1+\Delta_r)|x|\right),
\end{aligned} \tag{18}$$

where $w = |x|/t$ and $t' = t\tau$, and the final form is obtained by employing the saddle point method [77] and the assumption that the saddle point of the function $\Theta = \Theta(\tau,w) = \tau[r + (w/\tau)/(2D/U_0) + \Phi(1,w/\tau)]$, defined by $0 = [\mathrm{d}\Theta(\tau,w)/\mathrm{d}\tau]|_{\tau=\tau_0}$ occurs within the unit interval. The symbol $\approx$ shows that the integral is approximated (by using the saddle point method). The physical implication of this result is that successive reset events prompt the PDF $p_{\mathrm{r}}(x,t)$ to relax to a steady profile determined exclusively by the resetting rate r. However, this profile is limited to a 'light cone' region demarcated by the saddle point τ_0, i.e., for $|x| < U_0\Delta_r t$. The linear growth of this region implies that eventually relaxation is achieved on the entire stretch of the axis. However, at any intermediate time, the region outside the light cone region has not yet relaxed. In other words, if the saddle point occurs outside the unit interval, then the minimum of $\Theta(\tau,w)$ at the end of the interval at $\tau = 1$ makes the dominant contribution to the integral. These results are succinctly summarised as

$$p_r(x,t) \sim \mathrm{e}^{-t\, I_r(x/t)}, \tag{19}$$

where the LDF reads

$$I_r(x/t) = \begin{cases} \dfrac{U_0}{2D}(1+\Delta_r)|x|/t, & |x| < U_0\Delta_r t \\ r + \dfrac{U_0^2}{4D} + \dfrac{x^2/t^2}{4D} + \dfrac{U_0}{2D}\dfrac{|x|}{t}, & |x| > U_0\Delta_r t \end{cases} \tag{20}$$

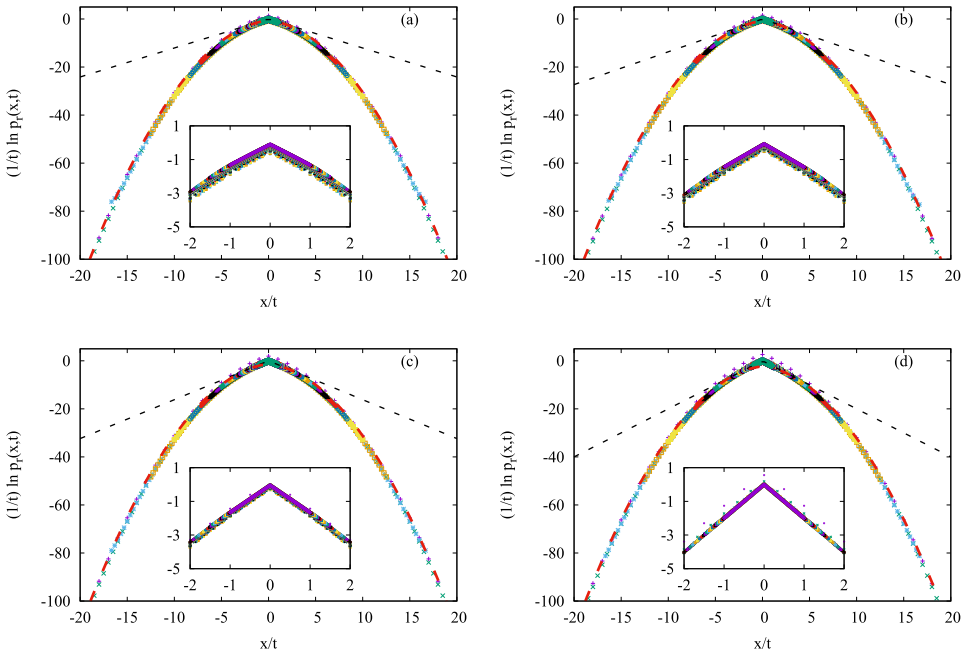

Figure 3. Graphs of the logarithm of the distribution function scaled by time, $(1/t)\ln p_r(x,t)$, vs x/t for Brownian motion in the potential $V(x) = U_0|x|$, for different resetting rates: (a) $r = 1/4$, (b) $r = 1/2$, (c) $r = 1$, (d) $r = 2$. The other parameters are $U_0 = 1$ and $D = 1$. The numerical calculations are performed by solving the equivalent Langevin equation, and the trajectories are recorded from $t = 0.1$ to $t = 5$ in units of $\Delta t = 0.1$. The distributions are calculated using the numerical inverse Laplace transform algorithm in Mathematica [73]. The black dotted line indicates the LDF calculated in equation (20) for different rates r for the case $|x| < U_0\Delta_r t$. The red dashed line is the base curve to which all the time-dependent forms collapse, following equation (20) for $|x| > U_0\Delta_r t$. The inset in figure shows a blowup of the solution near the origin, exhibiting exponentially decaying tails at long times.

This result also fixes the critical exponent, $\nu = 1$, implying that the relaxation ($\xi(t) \sim t$) occurs faster compared to diffusion ($\xi(t) \sim \sqrt{t}$). Numerical calculations of the PDF $p_r(x,t)$ via Laplace inversion corroborate our analytical results. For parameter values $D = 1$ and $U_0 = 1$ we plot $(1/t)\ln p_r(x,t)$ as a function of x/t for different values of the resetting rate r in figure 3. The collapse of the curves $p_r(x,t)$ at different times t onto a single master curve implies that there is a qualitative change in the nature of the distribution, demarcating the regions in which relaxation has been achieved from those in which the system is still in transient. Alternatively, if we look at a fixed location on the real line, there is a change in the nature of the PDF at that location as a function time. In other words, the system relaxes from its transient behaviour to its fixed point undergoing a dynamical phase transition. Here we note that for $U_0 = 0$ the LDF coincides with the one obtained in [74] for a free Brownian motion with stochastic resetting.

3.2. The asymmetric case: $x_0 \neq 0$

Let us now relax the condition that the reset location is placed symmetrically between the two branches of the potential, i.e., x_0 is no longer zero. In order to analyse the relaxation

behaviour in the asymmetric case with $x_0 > 0$, we need to know the density profile $\tilde{p}_0(x,s)$ in the absence of resetting, which follows from equation (10) in a straightforward manner using $r = 0$. Furthermore, the analysis of the asymmetric case is analogous to symmetric case discussed in the previous subsection, and hence we describe the essential steps addressing the spatial region $x \geqslant x_0$, in which the density profile reads

$$\begin{aligned}
\tilde{p}_0^{x\geqslant x_0}(x,s) &= \frac{\mathrm{e}^{\frac{U_0}{2D}[x_0-(1+\Delta_s)x]}}{U_0\Delta_s(\Delta_s-1)}[\Delta_s \mathrm{e}^{\frac{U_0 x_0 \Delta_s}{2D}} - 2\ \sinh(U_0 x_0 \Delta_s/2D)] \\
&= \frac{U_0}{4D}\mathrm{e}^{-\frac{U_0}{2D}(x-x_0)}\frac{1}{s}\left[(\Delta_s+1)\mathrm{e}^{-\frac{U_0}{2D}\Delta_s(x-x_0)}\right. \\
&\quad \left. - \frac{\Delta_s+1}{\Delta_s}\mathrm{e}^{-\frac{U_0}{2D}\Delta_s(x-x_0)} + \frac{\Delta_s+1}{\Delta_s}\mathrm{e}^{-\frac{U_0}{2D}\Delta_s(x+x_0)}\right] \\
&= \frac{U_0}{4D}\mathrm{e}^{-\frac{U_0}{2D}(x-x_0)}\frac{1}{s}\left[\left\{1-\frac{\partial}{\partial\frac{U_0}{2D}(x-x_0)}\right\}\mathrm{e}^{-\frac{U_0}{2D}\Delta_s(x-x_0)}\right. \\
&\quad - \left\{1-\frac{\partial}{\partial\frac{U_0}{2D}(x-x_0)}\right\}\frac{\mathrm{e}^{-\frac{U_0}{2D}\Delta_s(x-x_0)}}{\Delta_s} \\
&\quad \left. + \left\{1-\frac{\partial}{\partial\frac{U_0}{2D}(x+x_0)}\right\}\frac{\mathrm{e}^{-\frac{U_0}{2D}\Delta_s(x+x_0)}}{\Delta_s}\right]. \qquad (21)
\end{aligned}$$

From the inverse Laplace transform $\mathscr{L}^{-1}\{\exp(-U_0\Delta_s(x-x_0)/[2D])/\Delta_s\} = U_0/(2\sqrt{D\pi t})\exp(-[U_0^2/(4D)]t-(x-x_0)^2/[4Dt])$ (use the shift rule of the Laplace transform, $\mathscr{L}\{\mathrm{e}^{-at}f(t)\} = \tilde{F}(s+a)$ with $\tilde{F}(s) = \mathscr{L}\{f(t)\}$ and the formula $\mathscr{L}^{-1}\left\{s^{-1/2}\ \exp(-as^{1/2})\right\} = (\pi t)^{-1/2}\ \exp(-a^2/[4t])$ (see p. 258, formula 5.87 from reference [86]), the time domain representation of the density follows in the form

$$\begin{aligned}
p_0^{x\geqslant x_0}(x,t) &= \frac{U_0}{4D}\mathrm{e}^{-\frac{U_0}{2D}(x-x_0)}\left[\left\{1-\frac{\partial}{\partial\frac{U_0}{2D}(x-x_0)}\right\}\int_0^t \mathrm{d}t'\ \frac{x-x_0}{2\sqrt{\pi t'^3}}\mathrm{e}^{-\frac{U_0^2}{4D}t'-\frac{(x-x_0)^2}{4Dt'}}\right. \\
&\quad - \left\{1-\frac{\partial}{\partial\frac{U_0}{2D}(x-x_0)}\right\}\int_0^t \mathrm{d}t'\frac{U_0}{2\sqrt{\pi D t'}}\mathrm{e}^{-\frac{U_0^2}{4D}t'-\frac{(x-x_0)^2}{4Dt'}} \\
&\quad \left. + \left\{1-\frac{\partial}{\partial\frac{U_0}{2D}(x+x_0)}\right\}\int_0^t \mathrm{d}t'\frac{U_0}{2\sqrt{\pi D t'}}\mathrm{e}^{-\frac{U_0^2}{4D}t-\frac{(x+x_0)^2}{4Dt}}\right] \\
&\approx \frac{U_0}{4D}\mathrm{e}^{-\frac{U_0}{2D}(x-x_0)}\left(1+\frac{x+x_0}{U_0 t}\right)\mathrm{e}^{-t\Phi(1,\frac{x+x_0}{t})}, \qquad (22)
\end{aligned}$$

where we used the saddle point approximation in evaluating the last step, and $\Phi[\tau,\frac{a(x,x_0)}{t}] = \frac{U_0^2}{4D}\tau + \frac{[a(x,x_0)/t]^2}{4D\tau}$ with $a(x,x_0) = x \pm x_0$. To summarise, the long time behaviour

of the density profile in absence of resetting $p_0(x,t)$ reads

$$\tilde{p}_0(x,t) = \begin{cases} \dfrac{U_0}{4D}\left(1+\dfrac{x_0-x}{U_0 t}\right) \mathrm{e}^{-t[-\frac{U_0}{2D}(\frac{x+x_0}{t})+\Phi(1,\frac{x_0-x}{t})]}, & x \leqslant 0, \\ \dfrac{U_0}{4D}\left(1+\dfrac{x+x_0}{U_0 t}\right) \mathrm{e}^{-t[-\frac{U_0}{2D}(\frac{x_0-x}{t})+\Phi(1,\frac{x+x_0}{t})]}, & 0 \leqslant x \leqslant x_0, \\ \dfrac{U_0}{4D}\left(1+\dfrac{x+x_0}{U_0 t}\right) \mathrm{e}^{-t[\frac{U_0}{2D}(\frac{x-x_0}{t})+\Phi(1,\frac{x+x_0}{t})]}, & x_0 \leqslant x. \end{cases} \tag{23}$$

A casual look at equation (23) might tempt us to say that the long time behaviour of $p_0(x,t)$ is identical in regions $x \in [0, x_0]$ and $x \geqslant x_0$. However, it is to be noted that the argument of the exponential function behaves differently in the two regions. Furthermore, for $x_0 = 0$ the present result reduces to the previous density profile.

In order to understand the relaxation behaviour in presence of resetting for the asymmetric case, we once again invoke the renewal equation (16). As the nature of calculations is almost identical to the previously discussed symmetric case, we just quote the end results for the LDF defined in equation (19),

$$p_{r,x_0}(x,t) \sim \mathrm{e}^{-t\, I_{r,x_0}(x/t)}, \tag{24}$$

wherein the subscript x_0 is introduced as a reminder of the asymmetry. Furthermore, it is only the integral term of the renewal equation which contributes to the density profile $p_{r,x_0}(x,t)$ for reasons discussed in the previous subsection. Employing the saddle point approximation to evaluate the integral term in the renewal equation, we have:

(a) $x \leqslant 0$

$$I_{r,x_0}(x/t) = \begin{cases} \dfrac{U_0}{2D}\dfrac{x_0}{t}(\Delta_r - 1) - \dfrac{U_0}{2D}\dfrac{x}{t}(\Delta_r + 1), & \tau_0 < 1, \\ r + \dfrac{U_0^2}{4D} + \dfrac{1}{4D}\left(\dfrac{x-x_0}{t}\right)^2 - \dfrac{U_0}{2D}\dfrac{x+x_0}{t}, & \tau_0 > 1, \end{cases} \tag{25}$$

where $\tau_0 U_0 \Delta_r = \frac{x_0 - x}{t}$.

(b) $0 \leqslant x \leqslant x_0$

$$I_{r,x_0}(x/t) = \begin{cases} \dfrac{U_0}{2D}\dfrac{x_0}{t}(\Delta_r - 1) + \dfrac{U_0}{2D}\dfrac{x}{t}(\Delta_r + 1), & \tau_0 < 1, \\ r + \dfrac{U_0^2}{4D} + \dfrac{1}{4D}\left(\dfrac{x+x_0}{t}\right)^2 - \dfrac{U_0}{2D}\dfrac{x_0-x}{t}, & \tau_0 > 1, \end{cases} \tag{26}$$

where $\tau_0 U_0 \Delta_r = \frac{x_0 + x}{t}$.

(c) $x \geqslant x_0$

$$I_{r,x_0}(x/t) = \begin{cases} \dfrac{U_0}{2D}\dfrac{x_0}{t}(\Delta_r - 1) + \dfrac{U_0}{2D}\dfrac{x}{t}(\Delta_r + 1), & \tau_0 < 1, \\ r + \dfrac{U_0^2}{4D} + \dfrac{1}{4D}\left(\dfrac{x+x_0}{t}\right)^2 + \dfrac{U_0}{2D}\dfrac{x-x_0}{t}, & \tau_0 > 1, \end{cases} \tag{27}$$

where $\tau_0 U_0 \Delta_r = \frac{x_0 + x}{t}$.

For $x_0 = 0$, the region $x \in [0, x_0]$ does not contribute and the present result reduces to the previous case, with the LDF following equation (20).

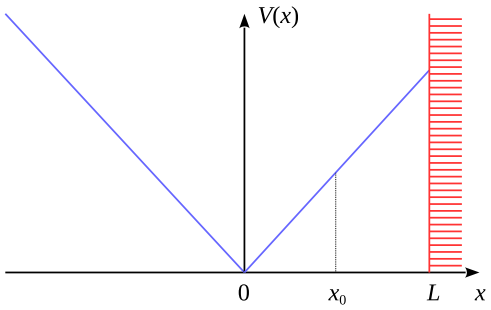

Figure 4. V-shaped potential centred about $x = 0$ with an absorbing boundary at $x = L$. The initial/resetting position of the particle is at $x = x_0$.

4. First-escape times from a V-shaped potential

In order to study the escape properties of a Brownian motion under resetting in a V-shaped potential, we introduce an absorbing boundary at a finite location from the origin, at $x = L$ (figure 4). The backward equation for the survival probability $q_r(x,t)$ of a diffusive particle in a potential at time t, having started at x_0 at $t = 0$ with resetting to the initial position reads [78]

$$\frac{\partial}{\partial t}q_r(x,t) = \left(-V'(x)\frac{\partial}{\partial x} + D\frac{\partial^2}{\partial x^2}\right) q_r(x,t) - rq_r(x,t) + rq_r(x_0,t), \tag{28}$$

with the potential $V = V(x)$ given in (2). The initial condition is $q_r(x,0) = 1$ and the boundary condition $q_r(L,t) = 0$. One of the important questions that arise when considering resetting is whether resetting facilitates the escape or delays it. The answer to this question comes from the CV of the first-passage times in the absence of resetting [60]. Resetting is advantageous when CV > 1. To understand this, we note that when CV, the ratio of standard deviation to mean, is larger than one, the fluctuations of the associated first-passage times about their mean are fairly strong, and resetting can help tame some of the fluctuations, aiding in a faster escape. Before considering resetting, let us briefly look at the case without resetting, i.e., $r = 0$.

4.1. The case without resetting ($r = 0$)

In absence of resetting, the backward equation reads

$$\frac{\partial}{\partial t}q(x,t) = \left(-V'(x)\frac{\partial}{\partial x} + D\frac{\partial^2}{\partial x^2}\right) q(x,t), \tag{29}$$

where $q(x,t)$ is the survival probability in absence of resetting. The solution to the above equation in Laplace domain reads

$$\tilde{q}(x,s) = \begin{cases} a_- \mathrm{e}^{-m_- x} + \dfrac{1}{s}, & x \leqslant 0 \\ b_+ \mathrm{e}^{m_+ x} + b_- \mathrm{e}^{m_- x} + \dfrac{1}{s}, & 0 \leqslant x \leqslant L, \end{cases} \tag{30}$$

where $m_\pm = \frac{U_0}{2D}(1 \pm \Delta_s)$ and $\Delta_s = \sqrt{1 + \frac{4sD}{U_0^2}}$. Continuity of the solution and its derivative at $x = 0$ gives us the following equations connecting the parameters,

$$a_- = b_+ + b_-, \tag{31a}$$

$$-m_- a_- = b_+ m_+ + b_- m_-. \tag{31b}$$

Using the absorbing boundary at $x = L$ results in

$$b_- = \frac{1}{s}\left(\frac{2m_- \mathrm{e}^{m_+ L}}{m_+ + m_-} - \mathrm{e}^{m_- L}\right)^{-1} = \frac{1}{s}\frac{\exp\left(-\frac{U_0 L}{2D}\right)}{2\ \sinh\left(\frac{U_0 L \Delta_s}{2D}\right) - \Delta_s\ \exp\left(\frac{U_0 L \Delta_s}{2D}\right)}, \tag{32a}$$

$$b_+ = -\frac{2m_-}{m_+ + m_-} b_- = \frac{\Delta_s - 1}{s}\frac{\exp\left(-\frac{U_0 L}{2D}\right)}{2\ \sinh\left(\frac{U_0 L \Delta_s}{2D}\right) - \Delta_s\ \exp\left(\frac{U_0 L \Delta_s}{2D}\right)}, \tag{32b}$$

$$a_- = b_+ + b_- = \frac{\Delta_s}{s}\frac{\exp\left(-\frac{U_0 L}{2D}\right)}{2\ \sinh\left(\frac{U_0 L \Delta_s}{2D}\right) - \Delta_s\ \exp\left(\frac{U_0 L \Delta_s}{2D}\right)}. \tag{32c}$$

Substituting this into equation (30) leads to the expression for the survival probability $\tilde{q}(x, s)$. Now, if the distribution of the first-passage times is F, in Laplace domain we have

$$\tilde{F}(x,s) = 1 - s\tilde{q}(x,s) = \begin{cases} \dfrac{\Delta_s\ \exp\left(-\frac{U_0}{2D}\{L + x(1-\Delta_s)\}\right)}{\Delta_s\ \exp\left(\frac{U_0 L \Delta_s}{2D}\right) - 2\ \sinh\left(\frac{U_0 L \Delta_s}{2D}\right)}, & x \leqslant 0, \\ \mathrm{e}^{\frac{U_0}{2D}(x-L)}\dfrac{\Delta_s\ \exp\left(\frac{U_0 x \Delta_s}{2D}\right) - 2\ \sinh\left(\frac{U_0 x \Delta_s}{2D}\right)}{\Delta_s\ \exp\left(\frac{U_0 L \Delta_s}{2D}\right) - 2\ \sinh\left(\frac{U_0 L \Delta_s}{2D}\right)}, & 0 \leqslant x \leqslant L. \end{cases} \tag{33}$$

The piecewise nature of the distribution takes care of the initial location of the particle, and gives us the probability that it is absorbed at $x = L$. Choosing the initial location of the particle on the negative x-axis, we find that the mean escape time to the absorbing boundary is

$$\langle \tau(x, L)\rangle = -\lim_{s\to 0}\frac{\partial}{\partial s}\tilde{F}(x,s) = \frac{2D}{U_0^2}\left[\mathrm{e}^{\frac{U_0 L}{D}} - 1 - \frac{U_0}{2D}(x + L)\right], \quad x < 0. \tag{34}$$

Furthermore, we obtain

$$\langle \tau(x, L)\rangle = \frac{2D}{U_0^2}\left[\mathrm{e}^{\frac{U_0 L}{D}} - e^{\frac{U_0 x}{D}} - \frac{U_0}{2D}(L - x)\right], \quad 0 < x < L. \tag{35}$$

The second moment $\langle \tau^2(x, L)\rangle = \lim_{s\to 0}\frac{\partial^2}{\partial s^2}\tilde{F}(x, s)$ becomes

$$\begin{aligned} \langle \tau^2(x, L)\rangle = \frac{4D^2}{U_0^4}\Bigg\{ &\left(2\ \mathrm{e}^{\frac{2U_0 L}{D}} - \mathrm{e}^{\frac{U_0 L}{D}} - 1\right) \\ &- \frac{U_0}{2D}\left[\left(6\ \mathrm{e}^{\frac{U_0 L}{D}} - 1\right)L + \left(2\ \mathrm{e}^{\frac{U_0 L}{D}} - 1\right)x\right] \\ &+ \frac{U_0^2}{4D^2}(x + L)^2\Bigg\}, \quad x < 0, \end{aligned} \tag{36}$$

and

$$\langle\tau^2(x,L)\rangle = \frac{4D^2}{U_0^4}\left\{\left(1+2\,\mathrm{e}^{\frac{U_0L}{D}}\right)\left(\mathrm{e}^{\frac{U_0L}{D}}-\mathrm{e}^{\frac{U_0x}{D}}\right)\right.$$
$$-\frac{U_0}{2D}\left[\left(6\,\mathrm{e}^{\frac{U_0L}{D}}-2\,\mathrm{e}^{\frac{U_0x}{D}}+1\right)L-\left(2\,\mathrm{e}^{\frac{U_0L}{D}}+2\,\mathrm{e}^{\frac{U_0x}{D}}+1\right)x\right]$$
$$\left.+\frac{U_0^2}{4D^2}(L-x)^2\right\},\quad 0<x<L. \tag{37}$$

In order to evaluate the limits we have used the fact that for s approaching 0, Δ_s approaches unity.

4.1.1. Coefficient of variation. The coefficient of variation (CV) of a random variable X is defined as the ratio of its standard deviation to its mean, $\mathrm{CV} = \sqrt{\langle X^2\rangle - \langle X\rangle^2}/\langle X\rangle$. In the context of first-passage times, the CV helps determine whether resetting can facilitate the completion of a stochastic process or rather slows it down [60]. In other words if the magnitude of fluctuations is dominant relative to the mean, i.e., $\mathrm{CV} > 1$, then resetting can be employed to reduce these fluctuations, thereby aiding in the escape to an absorbing boundary. In contrast, $\mathrm{CV} < 1$ means that resetting does not have any significant advantage. In order to address this aspect, let us introduce dimensionless parameters $\mu = \frac{U_0L}{2D}$, the ratio of energy barrier to temperature, and $z = \frac{x}{L}$, the dimensionless initial position in terms of the distance of the absorbing wall from the origin. Furthermore, the dynamics of a Brownian particle governed by the parameters D and U_0 introduces a natural time-scale $2D/U_0^2$, in terms of which all relevant times can be measured. Let us analyse the two cases with initial location on the negative and positive x-axis, respectively.

(a) $x < 0$: in terms of the dimensionless parameters μ and z we have

$$\frac{\langle\tau(x,L)\rangle}{2D/U_0^2} = \mathrm{e}^{2\mu} - 1 - \mu(1+z), \tag{38a}$$

$$\frac{\langle\tau^2(x,L)\rangle}{4D^2/U_0^4} = \left(2\,\mathrm{e}^{4\mu} - \mathrm{e}^{2\mu} - 1\right) - \mu\left(6\,\mathrm{e}^{2\mu} - 1\right)$$
$$-\mu z\left(2\,\mathrm{e}^{2\mu} - 1\right) + \mu^2(1+z)^2. \tag{38b}$$

Now,

$$\mathrm{CV}^2 = \frac{\langle\tau^2(x,L)\rangle}{\langle\tau(x,L)\rangle^2} - 1, \tag{39}$$

and thus $\mathrm{CV}^2 >=< 1$ transforms to $\langle\tau^2(x,L)\rangle - 2\langle\tau(x,L)\rangle^2 >=< 0$. Hence, the quantity of interest is the difference of the moments, and the resulting equation will help us demarcate the regions of the parameter space where resetting is useful. It is simpler to look at the equation $0 = \langle\tau^2(x,L)\rangle - 2\langle\tau(x,L)\rangle^2$, which, substituting the expressions for the two moments, reads

$$-\mu^2(1+z)^2 + \mu z\left(2\,\mathrm{e}^{2\mu} - 3\right) - \mu\left(2\,\mathrm{e}^{2\mu} + 3\right) + 3\left(\mathrm{e}^{2\mu} - 1\right) = 0. \tag{40}$$

With the coefficient of z^2 having a negative sign, the parabola is concave downwards, and the roots $\{z_1(\mu), z_2(\mu)\}$ mark the regions of $\mathrm{CV} >< 1$. The concavity of the curve implies that $\mathrm{CV} > 1$ for $z_1(\mu) < z < z_2(\mu)$. However, for the physically interesting case $\mu > 1$, i.e., the barrier height exceeds thermal energy, none of the two roots exist for $z < 0$. This also implies

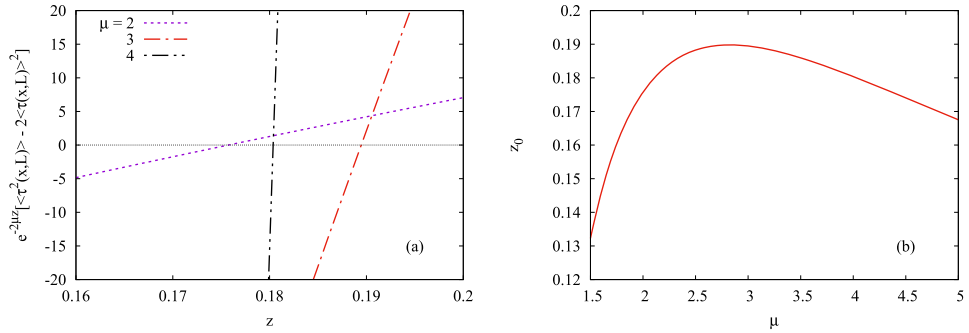

Figure 5. (a) Demonstration of the solution z_0 of equation (42), for the specific cases $\mu = 2, 3, 4$. The nonmonotonic behaviour of the zero crossing is clearly discernible from these graphs. (b) Location of the zero of $\langle \tau^2(x,L)\rangle - 2\langle \tau(x,L)\rangle^2$ for different values of μ.

that fluctuations in the distribution of first passage time are not strong enough to warrant any advantage when resetting is introduced in the dynamics of the system.

(b) $0 < x < L$: For the initial position on the positive x-axis,

$$\frac{\langle \tau(x,L)\rangle}{2D/U_0^2} = \mathrm{e}^{2\mu} - \mathrm{e}^{2\mu z} - \mu(1-z), \tag{41a}$$

$$\frac{\langle \tau^2(x,L)\rangle}{4D^2/U_0^4} = \left(2\,\mathrm{e}^{2\mu}+1\right)\left(\mathrm{e}^{2\mu}-\mathrm{e}^{2\mu z}\right) - \mu\left(6\,\mathrm{e}^{2\mu} - 2\,\mathrm{e}^{2\mu z}+1\right) + \mu z\left(2\,\mathrm{e}^{2\mu}+2\,\mathrm{e}^{2\mu z}+1\right) + \mu^2(1-z)^2. \tag{41b}$$

The condition $0 = \langle \tau^2(x,L)\rangle - 2\langle \tau(x,L)\rangle^2$ for the case of the initial position in the interval $(0,L)$ is

$$-\mu^2(1-z)^2 + \mu z\left(6\,\mathrm{e}^{2\mu z} - 2\,\mathrm{e}^{2\mu}+1\right) - \mu\left(2\,\mathrm{e}^{2\mu}+2\,\mathrm{e}^{2\mu z}+1\right) + \left(\mathrm{e}^{2\mu}-\mathrm{e}^{2\mu z}\right)\left(2\,\mathrm{e}^{2\mu z}+1\right) = 0. \tag{42}$$

Now, for physically significant cases, $\mu > 1$, and hence, we study the location of the zero z_0 of $\langle \tau^2(x,L)\rangle - 2\langle \tau(x,L)\rangle^2$ for a few representative values of the parameter μ in figure 5(a). Studying the variation of $\mathrm{e}^{-2\mu z}\,\mathrm{CV}^2$ for different values of μ, it is clear that the location of zero exhibits a nonmonotonic behaviour as a function of μ. To further corroborate this assertion, we study in figure 5(b) the variation of $z_0(\mu)$. It is observed from the figure that z_0 varies nonmonotonically as a function of the parameter μ, with the peak located around $\mu \approx 2.83$, and with the corresponding value of the reset location reading $z_0 \approx 0.1879$. It also becomes evident from the graphs that for $z > z_0$, $\mathrm{CV}^2 > 1$. In other words, for resetting positions in the interval $z \in (z_0, 1)$, resetting expedites the barrier escape to the absorbing wall at $x = L$.

4.2. The case with resetting ($r > 0$)

In the Laplace domain equation (28) now reads

$$s\tilde{q}_r(x,s) - 1 = \left(-V'(x)\frac{\partial}{\partial x} + D\frac{\partial^2}{\partial x^2}\right)\tilde{q}_r(x,s) - r\tilde{q}_r(x,s) + r\tilde{q}_r(x_0,s), \tag{43}$$

and thus

$$\tilde{q}_r(x,s) = \begin{cases} a_- \mathrm{e}^{-m_- x} + \dfrac{1 + r\tilde{q}(x_0,s)}{r+s}, & x \leqslant 0 \\ b_+ \mathrm{e}^{m_+ x} + b_- \mathrm{e}^{m_- x} + \dfrac{1 + r\tilde{q}(x_0,s)}{r+s}, & 0 \leqslant x \leqslant L, \end{cases} \tag{44}$$

where $m_\pm = \frac{U_0}{D}(1 \pm \Delta_{r+s})$. Using the continuity of the survival probability and its derivative at $x = 0$ along with the boundary condition $\tilde{q}_r(L,t) = 0$ we have

$$a_- = \frac{1 + r\tilde{q}(x_0,s)}{r+s} \frac{\Delta_{r+s}\ \exp\left(-\frac{U_0 L}{2D}\right)}{2\ \sinh\left(\frac{U_0 L \Delta_{r+s}}{2D}\right) - \Delta_{r+s}\ \exp\left(\frac{U_0 L \Delta_{r+s}}{2D}\right)}, \tag{45a}$$

$$b- = \frac{1 + r\tilde{q}(x_0,s)}{r+s} \frac{\exp\left(-\frac{U_0 L}{2D}\right)}{2\ \sinh\left(\frac{U_0 L \Delta_{r+s}}{2D}\right) - \Delta_{r+s}\ \exp\left(\frac{U_0 L \Delta_{r+s}}{2D}\right)}, \tag{45b}$$

$$b_+ = \frac{1 + r\tilde{q}(x_0,s)}{r+s} \frac{(\Delta_{r+s} - 1)\exp\left(-\frac{U_0 L}{2D}\right)}{2\ \sinh\left(\frac{U_0 L \Delta_{r+s}}{2D}\right) - \Delta_{r+s}\ \exp\left(\frac{U_0 L \Delta_{r+s}}{2D}\right)}. \tag{45c}$$

This allows us to write the survival probability $\tilde{q}_r$ under resetting in equation (44). Furthermore, for the case of resetting to the initial position, the survival probability can be determined in a self-consistent manner. As we have seen earlier, resetting is not useful for motion starting in the negative branch of the potential, and hence we do not pursue that case any further. Conversely, for initial locations in the positive branch, there is a finite subset of the interval $[0, L]$, in which resetting expedites the barrier crossing. Furthermore, the distribution of first-passage times $F(x,t)$ in the absence of resetting ($r = 0$) is connected with the survival probability under reset [32],

$$\tilde{q}_r(x,s) = \frac{1 - \tilde{F}(x, r+s)}{s + r\tilde{F}(x, r+s)}, \tag{46}$$

allowing us to calculate the mean escape time under resetting for the case $0 < x < L$,

$$\begin{aligned} \langle \tau_r(x,L) \rangle &= \frac{1 - \tilde{F}(x,r)}{r\tilde{F}(x,r)} \\ &= \frac{\exp\left(\frac{U_0}{2D}[L - x]\right)\left[\Delta_r\ \exp\left(\frac{U_0 \Delta_r\, L}{2D}\right) - 2\ \sinh\left(\frac{U_0 \Delta_r\, L}{2D}\right)\right]}{r\,\Delta_r\ \exp\left(\frac{U_0}{2D}\Delta_r x\right) - 2r\ \sinh\left(\frac{U_0\ \Delta_r\ x}{2D}\right)} - \frac{1}{r} \\ &= \frac{1}{r}\left(\mathrm{e}^{\mu(1-z)}\frac{f_\mu(1,r)}{f_\mu(z,r)} - 1\right), \end{aligned} \tag{47}$$

where we have reverted back to the dimensionless variables μ and z in the last line, with $f_\mu(z,r) = \Delta_r\ \mathrm{e}^{\mu z \Delta_r} - 2\ \sinh(\mu z \Delta_r)$. We study the behaviour of the mean first-passage time $\langle \tau_r(x,L) \rangle$ as a function of the resetting rate r in figure 6 for $\mu = 2$, We have also chosen the natural time-scale of the system as $2D/U_0^2 = 1$, which fixes $\Delta_r = \sqrt{1 + 2r}$. It is evident from figure 6 that $\langle \tau_r(x,L) \rangle$ exhibits a nonmonotonic dependence on r only when the reset location $z = x/L$ is above a certain threshold $z_0(\mu)$. Furthermore, in the region of reset locations,

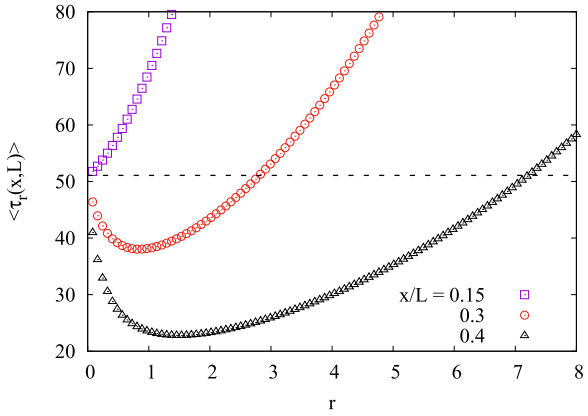

Figure 6. Mean first-passage time $\langle \tau_r(x,L)\rangle$ as a function of the resetting rate r, for $\mu = 2$. The nonmonotonic nature of the curve is evident from the figure. The dashed line shows the mean first-passage time $\langle \tau(x,L)\rangle$ in the absence of resetting.

i.e., for $z \in (z_0, 1)$, in which the mean escape time exhibits minima for a specific value of reset rate r_0, resetting indeed expedites the completion of the process, providing a significant advantage over diffusion-driven escape. In order to further our understanding of this behaviour, we study the behaviour of the extrema of the mean escape times.

To proceed let us look at the derivative of the mean escape time,

$$\begin{aligned}\frac{\mathrm{d}}{\mathrm{d}r}\langle \tau_r(x,L)\rangle &= \frac{1}{\Delta_r}\frac{\mathrm{d}}{d\Delta_r}\langle \tau_r(x,L)\rangle \\ &= \frac{4}{(\Delta_r^2-1)^2}\left[1-\mathrm{e}^{\mu(1-z)}\frac{f_\mu(1,r)}{f_\mu(z,r)}\right] \\ &\quad + \frac{2\ \mathrm{e}^{\mu(1-z)}}{\Delta_r(\Delta_r^2-1)}\frac{g_\mu(1,r)f_\mu(z,r)-f_\mu(1,r)g_\mu(z,r)}{f_\mu^2(z,r)},\end{aligned} \tag{48}$$

where $g_\mu(z,r) = \frac{\mathrm{d}}{\mathrm{d}\Delta_r} f_\mu(z,r) = (\mu z\Delta_r + 1)\mathrm{e}^{\mu z\Delta_r} - 2\ \mu z\ \cosh(\mu z\Delta_r)$. Now, at the location of the minima, we have $0 = \frac{\mathrm{d}}{\mathrm{d}r}\langle \tau_r(x,L)\rangle|_{r=r_0}$, implying that

$$\frac{2\Delta_{r_0}}{(\Delta_{r_0}^2-1)}\left[\frac{f_\mu(1,r_0)}{f_\mu(z,r_0)} - \mathrm{e}^{-\mu(1-z)}\right] = \frac{g_\mu(1,r_0)f_\mu(z,r_0)-f_\mu(1,r_0)g_\mu(z,r_0)}{f_\mu^2(z,r_0)}. \tag{49}$$

In order to assess the dependence of the optimal resetting rate r_0 on the reset position z we study the zero crossings of the two curves for different values of the parameter μ in figure 7(a). The nonmonotonic dependence on μ is observed here in the inset. In figure 7(b) we address the nature of the transition of the optimal resetting rate r_0 as function of the reset location z. The location $z_0(\mu)$ beyond which $r_0 > 0$ is obtained by extrapolating the $r_0(z)$ curve leading to $z_0(2) \approx 0.1757(3)$, $z_0(3) \approx 0.1895(3)$, and $z_0(4) \approx 0.1804(3)$ (entry in the parenthesis represents uncertainty in the final digit). The μ-dependent critical point $z_0(\mu)$ allows us to evaluate the critical exponent associated with the transition,

$$r_0 \sim (z - z_0(\mu))^{b(\mu)}, \tag{50}$$

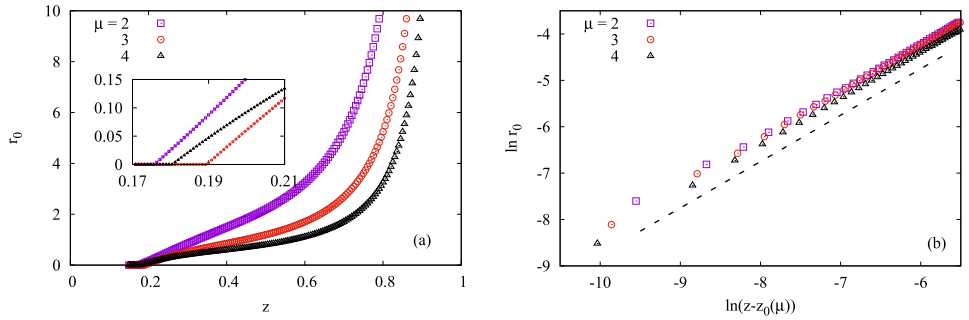

Figure 7. (a) Variation of the optimal resetting rate r_0 as a function of the reset location $z = x/L$. The inset shows a blowup of the region near the origin implying a continuous phase transition. (b) Phase transition of the optimal resetting rate r_0, with the black dashed line indicating slope 1.

with $b(2) \approx 0.979(4)$, $b(3) \approx 1.003(1)$, and $b(4) \approx 1.012(2)$. This implies that the optimal resetting rate r_0 exhibits a continuous phase transition with critical exponent $b \approx 1$ [63].

5. Summary

We studied the effects of stochastic resetting on the motion and the escape dynamics of a Brownian particle in a V-shaped confining potential. We found that resetting to a location other than the minima of the potential breaks the symmetry of the problem, in that a new peak is introduced in the PDF at the fixed reset location. Analysing the time dependent PDF we showed that the system relaxes to a non-equilibrium steady state via a dynamical phase transition, for which the LDF describing the transition exhibits a qualitative change in its behaviour. This demarcates the 'spacetime' into a 'light cone' within which the steady state has been achieved, and the size of this region grows linearly with time. In other words, relaxation to the steady state takes place faster than diffusion. Next we addressed the barrier escape problem when an absorbing barrier is introduced at a finite distance from the origin. We demonstrated that in the absence of any resetting, the relative fluctuations in the first-passage times are higher when the initial position is on the same side as the barrier, as compared to the opposite case. This implies that resetting expedites the completion of the process only when the reset location is on the same side as the absorbing wall. At an optimal rate, the mean escape time hits a minimum, providing a clear advantage over purely diffusion-driven escape. Furthermore, the optimal resetting rate exhibits a continuous transition as a function of the reset location, with a critical exponent of unity.

The present work has implications towards our current understanding about resetting mechanisms employed to molecular reaction systems. Since in many intracellular processes, running off at minute chemical concentrations, the first-reaction times are strongly defocused and the involved characteristic time scales may be orders of magnitude apart [79–81], the use of the mean reaction time is not justified and the full distribution of first-reaction times should be found—as we did in the present work. The simple setting considered in our work has provided us with an advantage to address the problem in an analytically tractable manner. However, we point out that instantaneous resetting is, of course, an idealisation. In addition, a constant resetting rate is one of the many possible mechanisms which can be employed to restart the motion. Another possible realistic scenario is to study the motion of a Brownian particle in a symmetric

confining potential, that is switched on and off stochastically, leading to resetting of the particle to the origin [82]. Finally, we note that the potential benefit of resetting in a potential may differ when the transport dynamics differs from Brownian motion in various anomalous diffusion scenarios [83]. Another interesting problem could be the investigation of random search process [84] in a confining potential and in the presence of a stochastic resetting. We plan to cover these aspects in future works.

Acknowledgments

RKS thanks Shlomi Reuveni for useful discussions and the financial support through SERB-MATRICS scheme Grant No. MTR/2019/000560. RM acknowledges financial support by German Science Foundation (DFG Grant ME 1535/7-1). RM also thanks the Foundation for Polish Science (Fundacja na rzecz Nauki Polskiej) for support within an Alexander von Humboldt Polish Honorary Research Scholarship. TS was supported by the Alexander von Humboldt Foundation.

Appendix A. Solution of equation (1) for resetting to the origin

Let us consider the case with $x_0 = 0$. Therefore, equation (1) with an initial condition at the origin, $p_r(x, t = 0) = \delta(x)$, and in the presence of the V-shaped potential (2) in the Laplace domain reads

$$s\tilde{p}_r(x,s) - \delta(x) = U_0 \frac{\partial}{\partial x}\left(\frac{\mathrm{d}|x|}{\mathrm{d}x}\tilde{p}_r(x,s)\right) + D\frac{\partial^2}{\partial x^2}\tilde{p}_r(x,s) - r\tilde{p}_r(x,s) + \frac{r}{s}\delta(x). \tag{A.1}$$

Since the problem is symmetric with respect to $x \to -x$, we substitute $y = |x|$ (so $y \geqslant 0$) and thus $\frac{\partial}{\partial x} f = [2\theta(x) - 1]\frac{\partial}{\partial y} f$ and $\frac{\partial^2}{\partial x^2} f = 2\delta(x)\frac{\partial}{\partial y} f + \frac{\partial^2}{\partial y^2} f$, to obtain

$$s\tilde{p}_r(y,s) - \delta(x) = 2U_0\,\delta(x)\tilde{p}_r(y,s) + U_0\frac{\partial}{\partial y}\tilde{p}_r(y,s) + 2D\delta(x)\frac{\partial}{\partial y}\tilde{p}_r(y,s) + D\frac{\partial^2}{\partial y^2}\tilde{p}_r(y,s) - r\tilde{p}_r(y,s) + \frac{r}{s}\delta(x). \tag{A.2}$$

From here we obtain the system of equations

$$D\frac{\partial^2}{\partial y^2}\tilde{p}_r(y,s) + U_0\frac{\partial}{\partial y}\tilde{p}_r(y,s) - (r+s)\tilde{p}_r(y,s) = 0, \tag{A.3}$$

$$\left(2D\frac{\partial}{\partial y}\tilde{p}_r(y,s) + 2U_0\tilde{p}_r(y,s)\right)\Big|_{y=0} + \frac{r}{s} = -1. \tag{A.4}$$

From (A.3) we find the solution in form

$$\tilde{p}_r(y,s) = C(s) \times \exp\left(-\frac{U_0}{2D}\left[1 + \sqrt{1 + \frac{4D(r+s)}{U_0^2}}\right] y\right), \tag{A.5}$$

while from (A.4) we find the constant $C(s)$,

$$C(s) = \frac{s^{-1}(r+s)}{U_0\left[\sqrt{1+\frac{4D(r+s)}{U_0^2}}-1\right]}. \tag{A.6}$$

Therefore, the solution becomes

$$\tilde{p}_r(x,s) = \frac{s^{-1}(r+s)}{U_0\left[\sqrt{1+\frac{4D(r+s)}{U_0^2}}-1\right]} \times \exp\left(-\frac{U_0}{2D}\left[1+\sqrt{1+\frac{4D(r+s)}{U_0^2}}\right]|x|\right), \tag{A.7}$$

from where we find that it is normalised since

$$\begin{aligned}\left\langle \tilde{x}^0(s)\right\rangle &= \int_{-\infty}^{\infty} \tilde{p}_r(x,s)\mathrm{d}x \\ &= \frac{4D}{U_0^2}\frac{s^{-1}(r+s)}{\left[\sqrt{1+\frac{4D(r+s)}{U_0^2}}-1\right]\left[\sqrt{1+\frac{4D(r+s)}{U_0^2}}+1\right]} = \frac{1}{s}.\end{aligned} \tag{A.8}$$

From the solution (A.7) in Laplace domain we have

$$\tilde{p}_r(x,s) = p_0(x,r+s) + s^{-1} r p_0(x,r+s), \tag{A.9}$$

where

$$\tilde{p}_0(x,r+s) = \frac{1}{U_0\left[\sqrt{1+\frac{4D(r+s)}{U_0^2}}-1\right]} \times \exp\left(-\frac{U_0}{2D}\left[1+\sqrt{1+\frac{4D(r+s)}{U_0^2}}\right]|x|\right). \tag{A.10}$$

Therefore, the solution becomes

$$p_r(x,t) = \mathrm{e}^{-r\,t} p_0(x,t) + \int_0^t r\ \mathrm{e}^{-rt'} p_0(x,t')\,\mathrm{d}t', \tag{A.11}$$

where

$$\begin{aligned} p_0(x,t) &= \mathscr{L}^{-1}\left\{\tilde{p}_0(x,s)\right\} \\ &= \mathscr{L}^{-1}\left\{\frac{1}{U_0\left[\sqrt{1+\frac{4Ds}{U_0^2}}-1\right]} \times \exp\left(-\frac{U_0}{2D}\left[1+\sqrt{1+\frac{4Ds}{U_0^2}}\right]|x|\right)\right\}. \end{aligned} \tag{A.12}$$

Multiplying and dividing this expression by $(\Delta_s + 1)$ yields ($\bar{\mu} = \frac{U_0|x|}{2D}$)

$$p_0(x,t) = \frac{U_0}{4D}\mathrm{e}^{-\bar{\mu}}\,\mathscr{L}^{-1}\left[s^{-1}\ \exp\left(-\bar{\mu}\sqrt{1+\frac{4Ds}{U_0^2}}\right)\right]$$

$$
\begin{aligned}
&- \frac{U_0}{4D}\mathrm{e}^{-\bar{\mu}}\frac{\partial}{\partial\bar{\mu}}\mathscr{L}^{-1}\left[s^{-1}\ \exp\left(-\bar{\mu}\sqrt{1+\frac{4Ds}{U_0^2}}\right)\right]\\
&= \frac{U_0}{4D}\mathrm{e}^{-\bar{\mu}}\int_0^t \frac{|x|}{\sqrt{4\pi Dt'^3}}\mathrm{e}^{-\frac{U_0^2}{4D}t'-\frac{x^2}{4Dt'}}\mathrm{d}t'\\
&\quad - \frac{U_0}{4D}\mathrm{e}^{-\bar{\mu}}\frac{\partial}{\partial\bar{\mu}}\int_0^t \frac{|x|}{\sqrt{4\pi Dt'^3}}\mathrm{e}^{-\frac{U_0^2}{4D}t'-\frac{x^2}{4Dt'}}\mathrm{d}t'\\
&= \frac{1}{2}\mathrm{e}^{-\bar{\mu}}\int_0^t \frac{\bar{\mu}}{\sqrt{4\pi Dt'^3}}\mathrm{e}^{-\frac{U_0^2}{4D}t'-\frac{D}{U_0^2t'}\bar{\mu}^2}\mathrm{d}t'\\
&\quad - \frac{1}{2}\mathrm{e}^{-\bar{\mu}}\frac{\partial}{\partial\bar{\mu}}\int_0^t \frac{\bar{\mu}}{\sqrt{4\pi Dt'^3}}\mathrm{e}^{-\frac{U_0^2}{4D}t'-\frac{D}{U_0^2t'}\bar{\mu}^2}\mathrm{d}t', \qquad \text{(A.13)}
\end{aligned}
$$

which together with equation (A.11) give the final result for the PDF.

In the long time limit ($s \to 0$) one finds

$$
\lim_{s\to 0} s\tilde{p}_r(x,s) \sim \frac{r}{U_0\left[\sqrt{1+\frac{4Dr}{U_0^2}}-1\right]} \times \exp\left(-\frac{U_0}{2D}\left[1+\sqrt{1+\frac{4Dr}{U_0^2}}\right]|x|\right), \qquad \text{(A.14)}
$$

which, from the final value theorem $\lim_{t\to\infty} p_r(x,t) = \lim_{s\to 0} s\tilde{p}_r(x,s)$, gives the stationary distribution

$$
p_{r,\mathrm{st}}(x) = \frac{r}{U_0\left[\sqrt{1+\frac{4Dr}{U_0^2}}-1\right]} \times \exp\left(-\frac{U_0}{2D}\left[1+\sqrt{1+\frac{4Dr}{U_0^2}}\right]|x|\right). \qquad \text{(A.15)}
$$

A graphical representation of the PDF (A.7) is provided in figures A1(a) and (b).

From equation (A.7) we find the MSD

$$
\begin{aligned}
\left\langle \tilde{x}^2(s)\right\rangle &= \frac{2(r+s)}{U_0 s\left[\sqrt{1+\frac{4D(r+s)}{U_0^2}}-1\right]}\int_0^\infty x^2 \times \exp\left(-\frac{U_0}{2D}\left[1+\sqrt{1+\frac{4D(r+s)}{U_0^2}}\right]|x|\right)\mathrm{d}x\\
&= \frac{32D^3}{U_0^4}\frac{s^{-1}(r+s)}{\left[\sqrt{1+\frac{4D(r+s)}{U_0^2}}-1\right]\left[\sqrt{1+\frac{4D(r+s)}{U_0^2}}+1\right]^3}\\
&= \frac{8D^2}{U_0^2}\frac{s^{-1}}{\left(\sqrt{1+\frac{4D(r+s)}{U_0^2}}+1\right)^2}. \qquad \text{(A.16)}
\end{aligned}
$$

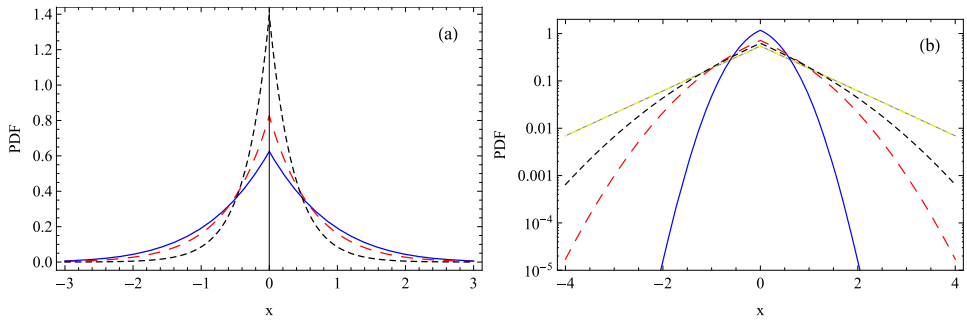

Figure A1. PDF (A.7) for (a) $t = 1$ and $r = 0.1$ (blue solid line), $r = 1$ (red dashed line), $r = 5$ (black dotted line); (b) for $r = 0.1$ and $t = 0.1$ (blue solid line), $t = 0.5$ (red dashed line), $t = 1$ (black dotted line), $t = 10$ (yellow dot-dashed line), which approaches the stationary distribution (A.15) (solid thin grey line). We note that the y-axis is represented on a logarithmic scale. We set $D = 1$ and $U_0 = 1$.

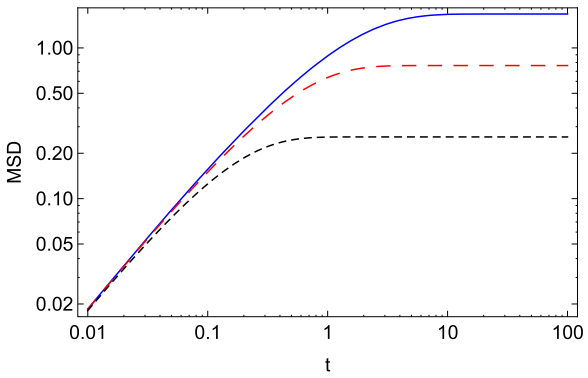

Figure A2. MSD (A.16) for $r = 0.1$ (blue solid line), $r = 1$ (red dashed line), $r = 5$ (black dotted line). We set $D = 1$ and $U_0 = 1$.

From the final value theorem, the long time limit ($t \to \infty$, i.e., $s \to 0$) reveals the saturation to the plateau value

$$\left\langle x^2(t)\right\rangle \sim \frac{8D^2}{U_0^2}\frac{1}{\left(1+\sqrt{1+\frac{4Dr}{U_0^2}}\right)^2}, \tag{A.17}$$

while the short time limit ($t \to 0$, i.e., $s \to \infty$) shows normal diffusion,

$$\left\langle x^2(t)\right\rangle \sim 2D\mathscr{L}^{-1}\left[\frac{s^{-1}}{s+r+\frac{U_0^2}{4D}}\right] = \frac{2D}{r+\frac{U_0^2}{4D}}\left[1-\mathrm{e}^{-\left(r+\frac{U_0^2}{4D}\right)t}\right] \sim 2Dt, \tag{A.18}$$

where we applied the Tauberian theorem [85]. A graphical representation of the MSD is shown in figure A2.

In absence of the potential, $U_0 = 0$, we have

$$\tilde{p}_r(x,s) = \frac{1}{2\sqrt{D}} s^{-1}(r+s)^{1/2} \times \exp\left(-\sqrt{\frac{r+s}{D}}|x|\right), \tag{A.19}$$

while the MSD becomes

$$\left\langle x^2(t)\right\rangle = 2D\mathscr{L}^{-1}\left[\frac{s^{-1}}{s+r}\right] = \frac{2D}{r}\left(1-\mathrm{e}^{-rt}\right), \tag{A.20}$$

as it should be for free diffusion with stochastic resetting [31].

Appendix B. Calculation of the LDF

The renewal equation (16) makes it clear that a complete understanding of motion in absence of any resetting is a prerequisite to fathom the dynamics under reset. The PDF in absence of any resetting is obtained by substituting $r = 0$ in equation (11), such that

$$\begin{aligned}\tilde{p}_0(x,s) &= \frac{1}{U_0(\Delta_s - 1)}\ \exp\left[-\frac{U_0}{2D}(1+\Delta_s)|x|\right] \\ &= \frac{U_0}{4D}\ \exp\left(-\frac{U_0}{2D}|x|\right)\frac{1}{s}\left[1 - \frac{\partial}{\partial(\frac{U_0}{2D}|x|)}\right]\exp\left(-\frac{U_0}{2D}|x|\Delta_s\right).\end{aligned} \tag{B.1}$$

Laplace inversion of the exponential term yields[5]

$$\begin{aligned} g(x,t) &\equiv \mathscr{L}^{-1}\left\{\exp\left(-\frac{U_0}{2D}|x|\Delta_s\right)\right\} \\ &= \mathscr{L}^{-1}\left\{\exp\left(-\frac{|x|}{\sqrt{D}}\left(s+\frac{U_0^2}{4D}\right)^{1/2}\right)\right\} \\ &= \mathrm{e}^{-\frac{U_0^2}{4D}t}\mathscr{L}^{-1}\left\{\exp\left(-\frac{|x|}{\sqrt{D}}s^{1/2}\right)\right\} \\ &= \frac{|x|}{\sqrt{4\pi D t^3}}\ \exp\left(-\frac{U_0^2}{4D}t - \frac{x^2}{4Dt}\right), \end{aligned} \tag{B.2}$$

where we apply the shift rule of the Laplace transform, $\mathscr{L}\{\mathrm{e}^{-at}f(t)\} = \tilde{F}(s+a)$, $\tilde{F}(s) = \mathscr{L}\{f(t)\}$ and $\mathscr{L}^{-1}\left\{\mathrm{e}^{-as^{1/2}}\right\} = \frac{a}{\sqrt{4\pi t^3}}\mathrm{e}^{-\frac{a^2}{4t}}$ (see, for example, p. 258, formula 5.85 from

[5] Here we note that the distribution of form $\wp_{\mathrm{fa}}(t) = \frac{|X|}{\sqrt{4\pi D t^3}}\ \exp\left(-\frac{X^2}{4Dt}\right)$ represents the Lévy–Smirnov distribution which occurs in the first arrival time density in one-dimensional Brownian search with δ-sink term at the origin $x = 0$, where X is the initial location of the searcher, see, for example [84]. Due to the exponential term $\mathrm{e}^{-\frac{U_0^2}{4D}t}$ the distribution (B.2) can be considered as an exponentially tempered Lévy–Smirnov distribution with tempering parameter $\frac{U_0^2}{4D}$. The tempering occurs due to the potential.

reference [86]). This allows us to write the density in time domain,

$$p_0(x,t) = \frac{U_0}{4D}\ \exp\left(-\frac{U_0}{2D}|x|\right)\left[1 - \frac{\partial}{\partial(\frac{U_0}{2D}|x|)}\right] h(x,t), \tag{B.3}$$

where

$$h(x,t) = \int_0^t \mathrm{d}t' g(x,t') = \frac{|x|}{\sqrt{4\pi D t}}\int_0^1 \mathrm{d}\tau \tau^{-3/2}\ \mathrm{e}^{-t\,\Phi(\tau,x/t)} = \frac{|x|}{\sqrt{4\pi D t}} h_0(x,t), \tag{B.4}$$

with $t' = t\tau$ and

$$\Phi(\tau, x/t) = \frac{U_0^2}{4D}\tau + \frac{x^2/t^2}{4D\tau}. \tag{B.5}$$

The integral defining h_0 is easily evaluated using the saddle point method [77] [6] for large t and fixed x/t, and for the case when the saddle point of the integrand defined via $0 = \frac{\mathrm{d}}{\mathrm{d}\tau}\Phi(\tau, x/t)|_{\tau=\tau_0}$ occurs within the unit interval, leads to $h(x,t) = \mathrm{e}^{-U_0|x|/2D}$, resulting in

$$p_0(x,t) = \frac{U_0}{2D}\mathrm{e}^{-U_0|x|/D}, \tag{B.6}$$

which is nothing but the stationary distribution in the potential $V(x) = U_0|x|$. However, this density profile is never realised in practice when the particle is constantly reset to its initial location at the origin, as resetting events prevent the particle to settle down to its characteristic form (B.6). And hence, it is not the saddle point at $\tau = \tau_0$ of the function Φ which makes the dominant contribution to h, but rather its minimal value at $\tau = 1$, leading to

$$h(x,t) = \mathrm{e}^{-t\Phi(1,x/t)}. \tag{B.7}$$

Now, using this result in equation (B.3) we have

$$p_0(x,t) = \frac{U_0}{4D}\mathrm{e}^{-\frac{U_0}{2D}|x|}(1 + |x|/U_0 t)\mathrm{e}^{-t\,\Phi(1,x/t)}, \tag{B.8}$$

finally providing us the distribution $p_r(x,t)$ in presence of resetting via the renewal equation,

$$\begin{aligned} p_r(x,t) &= \mathrm{e}^{-rt}p_0(x,t) + \int_0^t \mathrm{d}t' r\ \mathrm{e}^{-rt'}p_0(x,t') \\ &= \frac{U_0}{4D}\mathrm{e}^{-U_0|x|/2D}\left(1 + \frac{|x|}{U_0 t}\right)\mathrm{e}^{-t[r+\Phi(1,x/t)]} \end{aligned}$$

[6] The integral $I = \int_0^1 \mathrm{e}^{-tf(z)}g(z)\mathrm{d}z$ for large t can be approximated by

$$I \approx \mathrm{e}^{-t\,f(z_0)}g(z_0)\sqrt{\frac{2\pi}{tf''(z_0)}},$$

where z_0 is the saddle point of the function $f(z)$, i.e., $f'(z_0) = 0$, and if the saddle point is within the integration limits ($z_0 < 1$). If the saddle point is outside the integration limits ($z_0 > 1$), then the approximation result is calculated at $z_0 = 1$.

$$
\begin{aligned}
&+\frac{U_0 r}{4D}\int_0^t \mathrm{d}t'\left(1+\frac{|x|}{U_0 t'}\right)\mathrm{e}^{-t'\left[r+\frac{|x|/t'}{2D/U_0}+\Phi(1,x/t')\right]}\\
&=\frac{U_0}{4D}\mathrm{e}^{-U_0|x|/2D}\left(1+\frac{|x|}{U_0 t}\right)\mathrm{e}^{-t[r+\Phi(1,x/t)]}\\
&+\frac{U_0 rt}{4D}\int_0^1 \mathrm{d}\tau\left(1+\frac{w}{U_0\tau}\right)\mathrm{e}^{-t'\Theta(\tau,w)},
\end{aligned}
\tag{B.9}
$$

where $w=|x|/t$ and

$$
\Theta(\tau,w)=\tau\left[r+\frac{w/\tau}{2D/U_0}+\Phi(1,w/\tau)\right]=\left(r+\frac{U_0^2}{4D}\right)\tau+\frac{w^2}{4D}\frac{1}{\tau}+\frac{U_0 w}{2D}.
\tag{B.10}
$$

Now, unlike the case of $p_0(x,t)$, where only the time dependent form of the density profile is of interest to us, for $p_r(x,t)$ we want to know both the transient as well as the steady state solutions. First let us look at the steady state behaviour. As can be seen from the second term defining $p_r(x,t)$, the dominant contribution to the integral comes from the saddle point of the argument of the exponential $\Theta(\tau,w)$, defined as: $0=\frac{\mathrm{d}}{\mathrm{d}\tau}\Theta(\tau,w)|_{\tau=\tau_0}\Rightarrow\tau_0=w/U_0\Delta_r$. As a result,

$$
\begin{aligned}
t\int_0^1 \mathrm{d}\tau\left(1+\frac{w}{U_0\tau}\right)\mathrm{e}^{-t'\,\Theta(\tau,w)} &\approx \sqrt{\frac{4\pi D}{|x|U_0^3\Delta_r^3}}(1+\Delta_r)\\
&\quad\times\exp\left(-t\left[\frac{U_0}{2D}(1+\Delta_r)\frac{|x|}{t}\right]\right).
\end{aligned}
\tag{B.11}
$$

This implies that the probability density in presence of resetting reads

$$
\begin{aligned}
p_r(x,t)&=\frac{U_0}{4D}\mathrm{e}^{-U_0|x|/2D}\left(1+\frac{|x|}{U_0 t}\right)\mathrm{e}^{-t\,[r+\Phi(1,x/t)]}\\
&\quad+\sqrt{\frac{4\pi D}{|x|U_0^3\Delta_r^3}}(1+\Delta_r)\exp\left(-t\left[\frac{U_0}{2D}(1+\Delta_r)\frac{|x|}{t}\right]\right)\\
&\sim\exp\left(-tI_r\left(\frac{x}{t}\right)\right),
\end{aligned}
\tag{B.12}
$$

where the last line follows from the fact that the first term eventually vanishes in long time limit. The final expression allows us to write the LDF,

$$
I_r\left(\frac{x}{t}\right)=\frac{U_0}{2D}(1+\Delta_r)\frac{|x|}{t},\quad \tau_0<1.
\tag{B.13}
$$

The implication of this result is that the steady state is achieved within a light cone region demarcated by the boundary $\tau_0<1$. Within this region of spacetime, sufficiently many resetting events have taken place so as to average out the fluctuations arising due to resetting and thus allowing the system to relax. However, this is only part of the entire region, and outside of the light cone the system is still transient. In this transient regime, $\tau_0>1$, thus making

the dominant contribution to the integral come from the point at which the argument of the exponential is minimal, $\tau = 1$, and as a consequence,

$$p_r(x,t) \approx \frac{U_0}{4D}(1+rt)\mathrm{e}^{-t\,\Theta(1,x/t)} \sim \mathrm{e}^{-t\,I_r(x/t)}, \tag{B.14}$$

as the long term behaviour is dominated by the exponential term, and the corresponding LDF becomes

$$I_r\left(\frac{x}{t}\right) = r + \frac{U_0^2}{4D} + \frac{x^2/t^2}{4D} + \frac{U_0}{2D}\frac{|x|}{t}, \quad \tau_0 > 1. \tag{B.15}$$

In absence of any potential ($U_0 = 0$) the LDF (B.13) turns to $I_r(w) = \sqrt{\frac{r}{D}}|w|$, and the LDF (B.15) to $I_r(w) = r + \frac{w^2}{4D}$, where $w = x/t$ [74].

ORCID iDs

R K Singh https://orcid.org/0000-0002-2816-2218
R Metzler https://orcid.org/0000-0002-6013-7020
T Sandev https://orcid.org/0000-0001-9120-3847

References

[1] Redner S 2001 *A Guide to First Passage Processes* (Cambridge: Cambridge University Press)
[2] Palyulin V V, Blackburn G, Lomholt M A, Watkins N W, Metzler R, Klages R and Chechkin A V 2019 *New J. Phys.* **21** 103028
[3] Collins F C and Kimball G E 1949 Diffusion-controlled reaction rates *J. Colloid Sci.* **4** 425
[4] Metzler R, Oshanin G and Redner S (ed) 2014 *First-Passage Phenomena and Their Applications* (Singapore: World Scientific)
[5] Szabo A, Schulten K and Schulten Z 1980 *J. Chem. Phys.* **72** 4350
[6] Li G-W, Berg O G and Elf J 2009 *Nat. Phys.* **5** 294
[7] Kolesov G, Wunderlich Z, Laikova O N, Gelfand M S and Mirny L A 2007 *Proc. Natl Acad. Sci.* **104** 13948
[8] Bauer M and Metzler R 2013 *PLoS ONE* **8** e53956
[9] Pulkkinen O and Metzler R 2013 *Phys. Rev. Lett.* **110** 198101
[10] Fauchald P and Tveraa T 2003 *Ecology* **84** 282
[11] Beńichou O, Coppey M, Moreau M, Suet P-H and Voituriez R 2005 *Phys. Rev. Lett.* **94** 198101
[12] Lomholt M A, Koren T, Metzler R and Klafter J 2008 *Proc. Natl Acad. Sci. USA* **105** 11055
[13] Brockmann D and Helbing D 2013 *Science* **342** 1337
[14] Gross B, Zheng Z, Liu S, Chen X, Sela A, Li J, Li D and Havlin S 2020 arXiv:2003.08382
[15] Kramers H A 1940 *Physica* **7** 284
[16] Risken H 1989 *The Fokker-Planck Equation* (Berlin: Springer)
[17] Hänggi P, Talkner P and Borkovec M 1990 *Rev. Mod. Phys.* **62** 251
[18] Luby M, Sinclair A and Zuckerman D 1993 *Inf. Process. Lett.* **47** 4391
[19] Tong H, Faloutsos C and Pan J-Y 2008 *Knowl. Inf. Syst.* **14** 327
[20] Avrachenkov K, Piunovskiy A and Zhang Y 2013 *J. Appl. Probab.* **50** 960
[21] Reuveni S, Urbakh M and Klafter J 2014 *Proc. Natl Acad. Sci.* **111** 4391
[22] Bell W J 1991 *Searching Behavior: The Behavioral Ecology of Finding Resources* (London: Chapman and Hall)
[23] Bartumeus F and Catalan J 2009 *J. Phys. A: Math. Theor.* **42** 434002
[24] Berg O G, Winter R B and von Hippel P H 1981 *Biochemistry* **20** 6929
[25] Brockwell P J, Gani J and Resnick S I 1982 *Adv. Appl. Probab.* **14** 709
[26] Kyriakidis E G 1994 *Stat. Probab. Lett.* **20** 239

[27] Visco P, Allen R J, Majumdar S N and Evans M R 2010 *Biophys. J.* **98** 109
[28] Kumar B K and Arivudainambi D 2000 *Comput. Math. Appl.* **40** 1233
[29] Di Crescenzo A, Giorno V, Nobile A G and Ricciardi L M 2003 *Queueing Syst.* **43** 329
[30] Evans M R, Majumdar S N and Schehr G 2020 *J. Phys. A: Math. Theor.* **53** 193001
[31] Evans M R and Majumdar S N 2011 *Phys. Rev. Lett.* **106** 160601
[32] Reuveni S 2016 *Phys. Rev. Lett.* **116** 170601
[33] Evans M R and Majumdar S N 2011 *J. Phys. A: Math. Theor.* **44** 435001
[34] Evans M R, Majumdar S N and Mallick K 2013 *J. Phys. A: Math. Theor.* **46** 185001
[35] Evans M R and Majumdar S N 2014 *J. Phys. A: Math. Theor.* **47** 285001
[36] Christou C and Schadschneider A 2015 *J. Phys. A: Math. Theor.* **48** 285003
[37] Pal A, Kundu A and Evans M R 2016 *J. Phys. A: Math. Theor.* **49** 225001
[38] Nagar A and Gupta S 2016 *Phys. Rev.* E **93** 060102
[39] Eule S and Metzger J J 2016 *New J. Phys.* **18** 033006
[40] Pal A and Prasad V V 2019 *Phys. Rev.* E **99** 032123
[41] Pal A, Chatterjee R, Reuveni S and Kundu A 2019 *J. Phys. A: Math. Theor.* **52** 264002
[42] Tateishi A A, Ribeiro H V, Sandev T, Petreska I and Lenzi E K 2020 *Phys. Rev.* E **101** 022135
[43] Domazetoski V, Masó-Puigdellosas A, Sandev T, Méndez V, Iomin A and Kocarev L 2020 *Phys. Rev. Res.* **2** 033027
Dos Santos M A F 2020 *Fractal Fract.* **4** 28
[44] Bodrova A S, Chechkin A V and Sokolov I M 2019 *Phys. Rev.* E **100** 012120
[45] Chechkin A and Sokolov I M 2018 *Phys. Rev. Lett.* **121** 050601
[46] Bodrova A and Sokolov I M 2020 *Phys. Rev.* E **101** 052130
[47] Masó-Puigdellosas A, Campos D and Méndez V 2019 *Phys. Rev.* E **100** 042104
[48] Goldenfeld N G 1993 *Lectures on Phase Transitions and the Renormalization Group* (Reading, MA: Addison-Wesley)
[49] Binney J J, Dowrick N J, Fisher A J and Newman M E J 1992 *The Theory of Critical Phenomena: An Introduction to the Renormalization Group* (Oxford: Clarendon)
[50] Yeomans J M 1992 *Statistical Mechanics of Phase Transitions* (Oxford: Clarendon)
[51] Fisher M E 1998 *Rev. Mod. Phys.* **70** 653
[52] Hohenberg P C and Halperin B I 1977 *Rev. Mod. Phys.* **49** 435
[53] Folk R and Moser G 2006 *J. Phys. A: Math. Gen.* **39** R207
[54] Kuśmierz L, Majumdar S N, Sabhapandit S and Schehr G 2014 *Phys. Rev. Lett.* **113** 220602
[55] Durang X, Henkel M and Park H 2014 *J. Phys. A: Math. Theor.* **47** 045002
[56] Kuśmierz L and Godowska-Nowak E 2015 *Phys. Rev.* E **92** 052127
[57] Kampos D and Méndez V 2015 *Phys. Rev.* E **92** 062115
[58] Rotbart T, Reuveni S and Urbakh M 2015 *Phys. Rev.* E **92** 060101
[59] Mattos T, Mejía-Monasterio C, Metzler R and Oshanin G 2012 *Phys. Rev.* E **86** 031143
[60] Pal A and Reuveni S 2017 *Phys. Rev. Lett.* **118** 030603
[61] Ray S, Mondal D and Reuveni S 2019 *J. Phys. A: Math. Theor.* **52** 255002
[62] Ray S and Reuveni S 2020 *J. Chem. Phys.* **152** 234110
[63] Ahmad S, Nayak I, Bansal A, Nandi A and Das D 2019 *Phys. Rev.* E **99** 022130
[64] Masó-Puigdellosas A, Campos D and Méndez V 2019 *Phys. Rev.* E **99** 012141
[65] Samanta A and Ghosh S K 1992 *J. Chem. Phys.* **97** 9321
[66] Hynes J T 1985 *Annu. Rev. Phys. Chem.* **36** 573
[67] Metzler R and Klafter J 2000 *Chem. Phys. Lett.* **321** 238
[68] Metzler R and Klafter J 2000 *Phys. Rep.* **339** 1
[69] Berezhovskii A M, Szabo A, Rotbart T, Urbakh M and Kolomeisky A B 2016 *J. Phys. Chem.* B **121** 3437
[70] Robin T, Reuveni S and Urbakh M 2018 *Nat. Commun.* **9** 779
[71] Pal A 2015 *Phys. Rev.* E **91** 012113
[72] Roldán É and Gupta S 2017 *Phys. Rev.* E **96** 022130
[73] Mallet A 2000 *Numerical Inversion of Laplace Transform* (Wolfram Library Archive) Item 210–968
[74] Majumdar S N, Sabhapandit S and Schehr G 2015 *Phys. Rev.* E **91** 052131
[75] Touchette H 2009 *Phys. Rep.* **478** 1
[76] Evans M R and Majumdar S N 2018 *J. Phys. A: Math. Theor.* **51** 475003
[77] Arfken G B and Weber H J 2005 *Mathematical Methods for Physicists* 6th edn (Amsterdam: Elsevier)

[78] Gardiner C W 1985 *Handbook of Stochastic Methods for Physics, Chemistry and the Natural Sciences* (Berlin: Springer)
[79] Grebenkov D S, Metzler R and Oshanin G 2018 *Commun. Chem.* **1** 96
[80] Godec A and Metzler R 2016 *Phys. Rev.* X **6** 041037
[81] Grebenkov D S, Metzler R and Oshanin G 2019 *New J. Phys.* **21** 122001
[82] Mercado-Vásquez G, Boyer D, Majumdar S N and Schehr G 2020 arXiv:2007.15696
[83] Metzler R, Jeon J-H, Cherstvy A G and Barkai E 2014 *Phys. Chem. Chem. Phys.* **16** 24128
[84] Palyulin V V, Chechkin A V and Metzler R 2014 *Proc. Natl Acad. Sci.* **111** 2931
Palyulin V V, Chechkin A V and Metzler R 2014 *J. Stat. Mech.* P11031
[85] Feller W 1968 *An Introduction to Probability Theory and its Applications* vol 2 (New York: Wiley)
[86] Oberhettinger F and Badii L 1973 *Tables of Laplace Transforms* (Berlin: Springer)